15B.6 **RAPID INTENSITY CHANGE IN HURRICANE LILI (2002)**

Mélicie Desflots*
RSMAS, University of Miami, Miami, Florida

1. INTRODUCTION

Rapid intensity change in tropical cyclones is one of the most difficult problems in hurricane prediction today. Hurricane Lili (2002) went trough a rapid intensification (from a category 2 to category 4 hurricane in about 24 h) followed by a rapid weakening (from category 4 to a category 1 hurricane in less than 18 h) before landfall on the Louisiana coast. None of the operational numerical weather prediction (NWP) models were able to forecast the rapid intensity change in Hurricane Lili. Numerous studies have shown that the principal factors controlling the intensity changes are air-sea interactions, atmospheric environmental factors (e.g vertical wind shear, moisture distribution) and Hurricane internal dynamics. This numerical modelling study focuses on the evolution of the storm structure and the impact of the environmental flow on the rapid intensification and rapid weakening of Hurricane Lili.

2. METHODOLOGY

The high-resolution non-hydrostatic, 5th generation Pennsylvania State University-NCAR Mesoscale Model (MM5) is used in this study. We use four nested domains with 45, 15, 5, 1.67 km grid resolutions, respectively. The second, third and fourth inner domains are following the vortex (Tenerelli and Chen, 2001). All domains have 28 sigma levels with 9 sigma levels within the planetary boundary layer (PBL). The model initial and lateral boundary conditions are from the 1°x1° National Centers for Environmental Prediction (NCEP) global analysis fields. The sea surface temperature (SST) is from the SSM/I satellite data. The model is initialized at 0000 UTC, 1 October 2002 and integrated for 72 h. The initial vortex from the global analysis fields is much weaker than the National Huricane Center (NHC) best track. We use a vortex-relocation procedure similar to that used by Liu et al. (1997) to obtain an initial vortex as close as possible to the observation.

3. RESULTS

Hurricane Lili went trough a similar track of Hurricane Isidore (2002) in the Gulf of Mexico. The model simulated track is very close to the NHC best track (Fig.1a) except for a small deviation after 0000 UTC 3 October. The model simulation captured both the intensification and the weakening of Lili before landfall. However, the both the intensification and the weakening are slower in the model than in the observations.

Corresponding author address : Mélicie Desflots, MPO, RSMAS, University of Miami, Miami, FL, 33149. e-mail : mdesflots@rsmas.miami.edu.

After passing through the western Cuba, Lili went through a rapid intensification. The observed minimum sea level pressure (MSPL) decreases from 967 to 940 hPa in 24 h from 0000 UTC 2-3 October. The model simulated MSLP reached the minimum 948 hPa at about the same time as the observed storm (Fig. 1b). Lili then went through a dramatic weakening, with the MSLP increasing to 960 hPa in the next 12 h, in the central Gulf before the landfall at the Gulf coast. It was far enough from the land so that land surface is not a main factor in the weakening process at this time. The observed maximum surface wind speed (MWS) shows a similar large drop from the maximum of 65 to 40 m s^{-1} (Fig. 1c). The model simulated MSLP and MWS have a similar trend, but did not reached the observed intensity. The model simulated MWS is particularly weaker compared to the observations. It may be due to the lack of coupling to the ocean surface waves, which is shown in a recent fully coupled atmosphere-wave-ocean modelling study by Chen et al (2006).

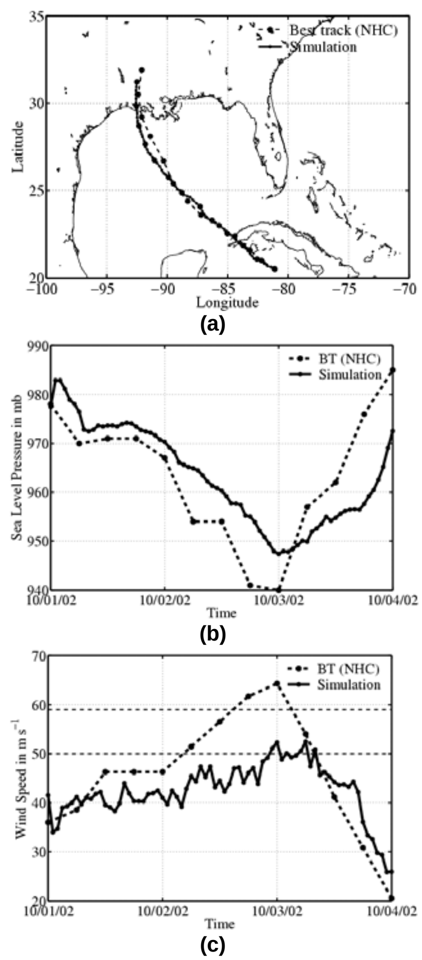

Figure 1 : (a) Track of Hurricane Lili, (b) Mean Sea Level Pressure (MSLP) in mb, (c) Wind speed for the 72 hours simulation. The solid line is the simulated storm and the dashed line is observed storm.

3.1 Rapid Intensification of Lili

To understand the processes responsible for Lili's rapid intensification, we conduct detailed analyses of the model simulated dynamic and thermodynamic fields. Figure 2 shows a time-height cross-section of potential temperature perturbation (from the 0000 UTC 2 October), relative humidity (RH) and equivalent potential temperature azimuthally and radially averaged at the radius of 18km where the aproximate location for the inner edge of the eyewall at the most intense stage is. The radius of maximum wind (RMW) varies from 50 km (at the beginning of the intensification) to about 25 km (smallest RMW of the simulation between 2-4 October). From the beginning of the intensification phase of Lili, the most significant warming occurs at the mid-levels between 3-7 km (Fig. 2a). Throughout the second day of the simulation, the warming region expands both upward and downward as its intensity increases. At the end of the October 2, the warming reaches about 3 K at 10 km height and the warming region of 2 K expands down to the surface. The RH (Fig. 2b) shows significant drying in the eye between 1200UTC October 2 to 0000UTC October 3. The eye is drying from the top down. The equivalent potential temperature illustrates the presence of two different air masses above and below the inversion layer as described in Willoughby (1998).

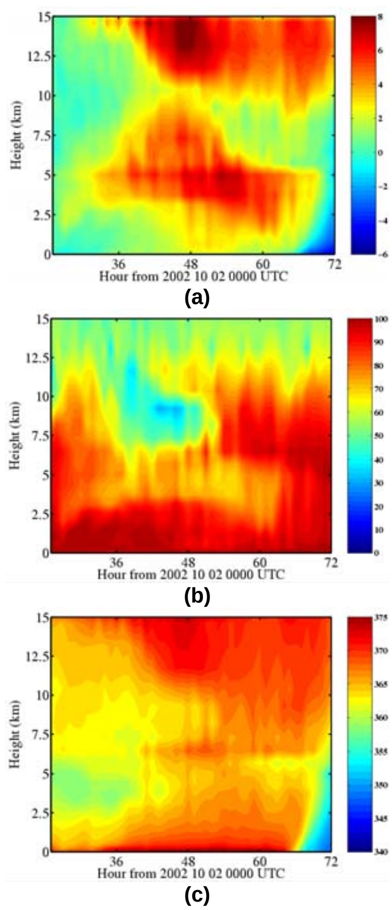

Figure 2 : Time-height cross-section for (a) $\Delta\theta$ from 0000 UTC 2 October in K, (b) RH in %, (c) θ_e in K from 0000 UTC 2 October to 0000UTC 4 October azimuthally and radially averaged over a circle of 18 km radius centred on the storm.

Below 3 km height, the warming rate is slower than above as shown by figure 3. As describe by previous studies the processes involved in the warming above and below 3 km (roughly at the inversion layer height) are different. Below the inversion layer, the warming is due to surface heat/moisture fluxes from the underlying warm ocean (Willoughby 1998). Above the inversion, the warming is due to forced dry descent in the eye to replace the air lost to the eyewall (Willoughby 1998). This warming leads to a rapid (slow) isobaric surface fall inside (outside) the radius of maximum winds (RMW). The largest isobaric fall located inside the RMW supports a peak of tangential winds tendency. At the beginning of the intensification stage, the azimuthally averaged tangential winds are weak and shallow (fig. 3d-f). As the warming area in the eye expands vertically, the vortex intensifies and expands vertically from the bottom to the top and the RMW moves inward.

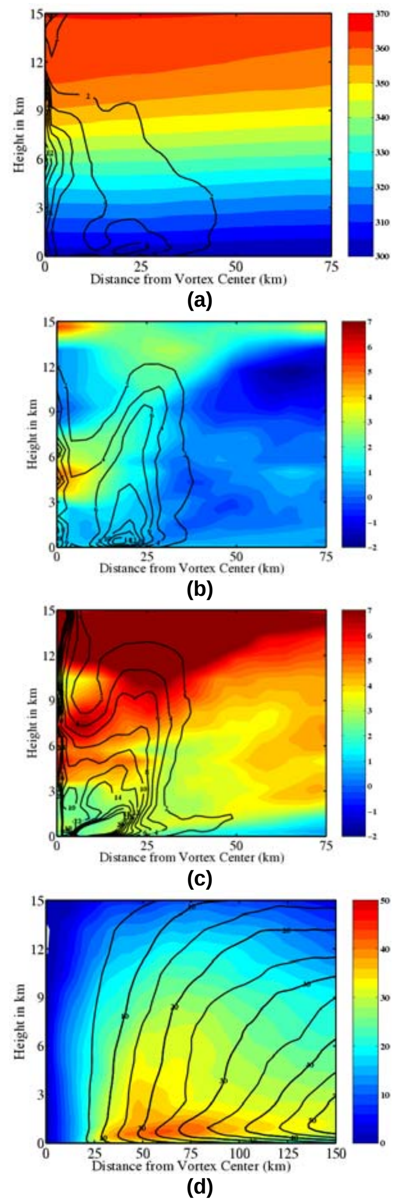

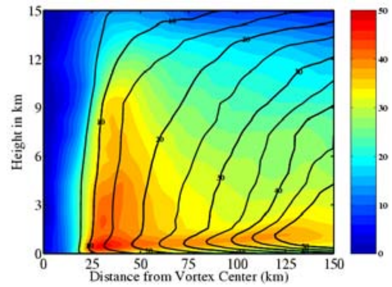

(e)

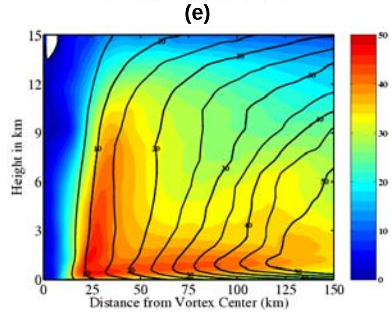

(f)

Figure 3 : Azimuthally averaged (a) θ at 0000 UTC 2 October (shaded) and inertial stability (black lines), (b)-(c) θ deviation from 0000 UTC 2 October at 1200 and 2200 UTC 2 October respectively (shaded) and inertial stability (black lines), (d)-(f) Tangential wind speed (shaded) and Absolute Angular Momentum (black lines) on 0000 UTC 2 October, 1200 and 2200 UTC 2 October respectively.

The upper-level low located to the north-west of Lili in the initial fields played a major role in both the intensification and the weakening of Lili (see fig. 3a-c). From 0000 UTC 1 October to 0000 UTC 3 October the storm is far enough south-east of the upper-low (which later merges into an upper-level trough fig. 4b) to not feel the vertical wind shear generated by this feature (fig. 5a). It even possibly enhanced the intensification of Lili during that stage as shown by different observational (Colon and Nightingale 1963, Bosart et al. 2000) and numerical studies on hurricane-trough interaction (Kimball and Evans 2002). Several physical mechanisms could explain the "positive" trough impact on Lili such as upper-level eddy angular momentum flux forcing (e.g., Molinaro and Vollaro 1989), enhanced upper-level divergence (Bosart et al. 2000; Shi et al. 1990) or superimposition of potential vorticity anomalies (Molinari et al. 1995, 1998).

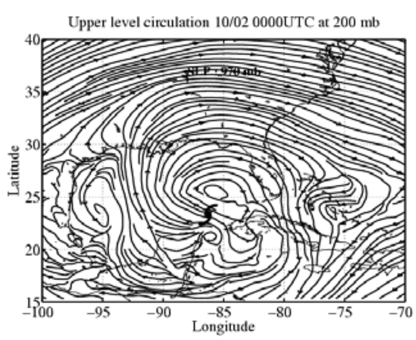

(a)

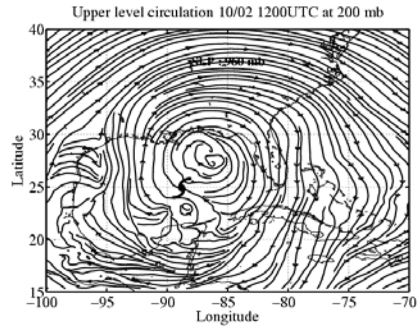

(b)

Figure 4 : (a)-(b) Streamlines at 200mb at 0000 UTC 2 October and 1200 UTC. The hurricane symbol represents the low level storm's center,

3.2 Weakening before landfall of Lili

As the storm gets closer to the trough, it starts to experience stronger upper-level westerlies (figs. 5a-b).

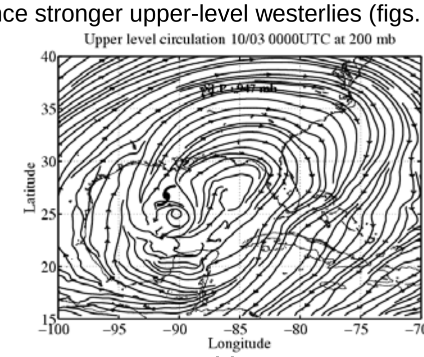

(a)

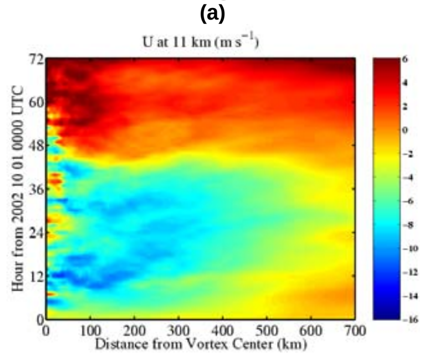

(b)

Figure 5 : (a) Streamlines at 200 hPa at 0000 UTC 3 October. The hurricane symbol represents the storm's center, (b) Time evolution of the meridionnal component of the wind from October 1-4.

The upper_level flow which was mostly easterly during the deepening phase of Lili turns to a westerly flow as the strom approaches the trough.

The storm both in the observations from TRMM/TMI and PR rainfall estimates and in the simulation evolves from a quasi-symmetric state on the 2 October (fig. 5a-b) to a really marked asymmetric state (in the left front quadrant- fig. 5c-e). Lili starts to show a significant and characteristic wave number one asymmetry in the rainfall field due to the vertical wind shear (e.g. Frank and Ritchie 1999, 2001; Black et al. 2002; Rogers et al. 2003). The shear magnitude between the 200 hPa and 850 hPa levels increases to almost 20 m s $^{-1}$ inside a radius of 100km centered on the storm.

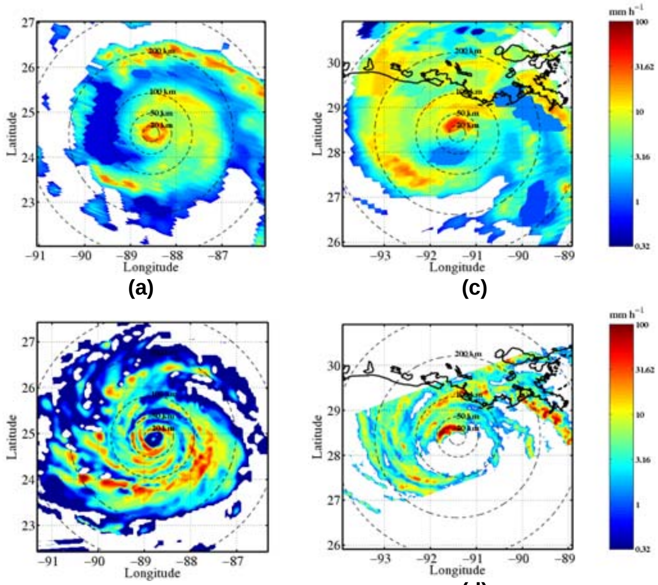

(a) (c)

(b) (d)

Figure 6 : Rainfall distribution in mm h^{-1}. (a) TRMM/TMI estimates at 1255 UTC 2 October 2002. (b) Model simulated rainfall at 1200 UTC 2 October 2002. (c)-(d) TRMM/TMI (PR) estimates at 0705 UTC 3 October 2002. (e) Model simulated rainfall at 0700 UTC 3 October 2002.

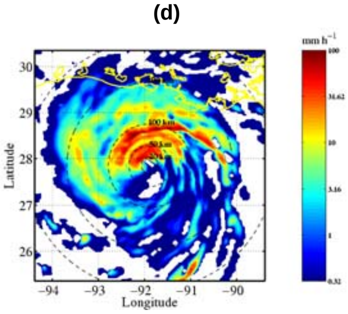

(e)

The combination of the North-western storm motion and a south-westerly vertical wind shear probably reinforced the wave number one asymmetry in the rainfall field. The azimuthally averaged environmental wind shear around the storm in an annulus of 200-700km centered around the storm and between the layer 200 hPa and 850 hPa is shown by figure 7. The averaged flow around the storm which was primarily south-easterly at all levels switches to a south-westerly flow at the upper-levels, therefore increasing the vertical wind shear over the storm.

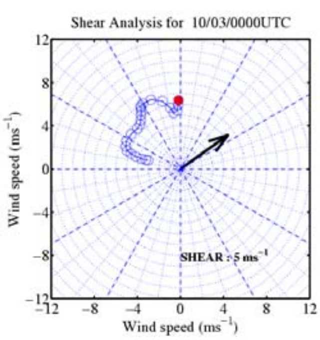

(a)

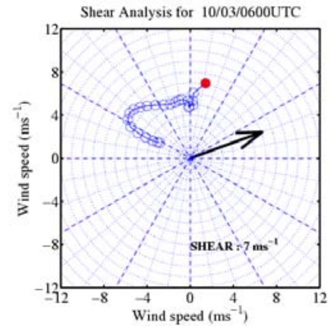

(b)

Figure 7 : Hodographs of the winds over the storm on (a) 0000 UTC 3 Octobe , (b) 0600 UTC 3 October. Each dot represents the horizontal wind vector averaged over and annulus of 200-700km around the storm at each vertical level. The red dot is the highest level and the black arrow is the mean vertical wind shear estimated as the difference between the averaged horizontal winds at 200hPa and 850hPa ($V_{h200hPa}$-$V_{h850hPa}$).

Several observational studies (e.g. Black et al. 2002) and numerical studies (e.g. Frank and Ritchie 1999,2001, Rogers et al. 2003) have described the impact of the vertical wind shear on hurricane intensity. Even weak vertical wind shear as low as 5 m s^{-1} has been shown to create some significant asymmetries in hurricanes and some induce significant weakening of the storm (e.g. Franck and Ritchie 2001). The warm temperature anomaly which was developing at mid and upper-levels during the intensification phase of Lili decreases, particularly at higher levels, under the influence of the vertical wind shear (fig 8a-b). The azimuthally averaged tangential wind speed which showed a peaked profile at the most intense stage of the simulated Lili (10/02 2200UTC) decays from the top down (fig 8c-d).

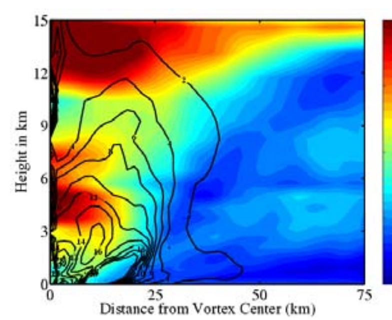

(a)

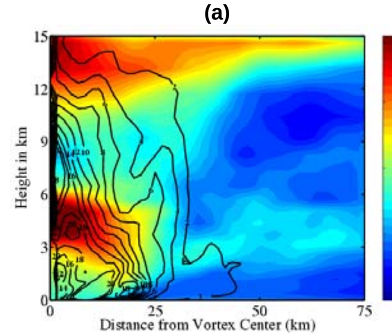

(b)

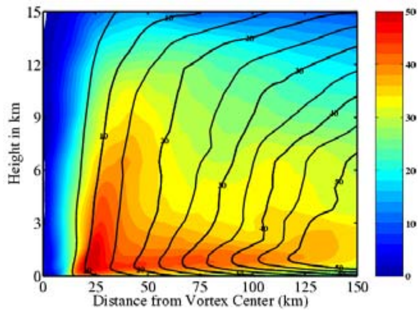

(c)

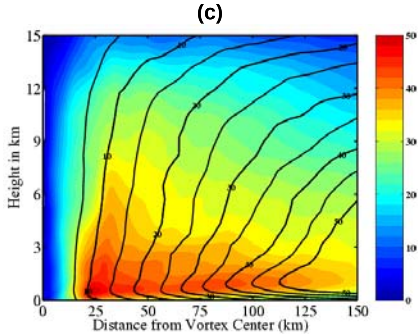

(d)

Figure 8 : Same as figure 3. (a)-(b) 0000 UTC October 3 and 0600 UTC respectively, (c)-(d) 0000 UTC and 0600 UTC 3 October respectively .

4. CONCLUSIONS

The environmental conditions at the upper-levels during the first 48 hours was particularly favourable for the rapid intensification or Hurricane Lili. The upper-level low/trough on the North-East side of the storm and the strong jet oriented from the North-West to the South-East on the eastern part of the storm helped to enhanced the outflow. Based on Willoughby's argument (1998), as the air from the eyewall is more efficiently "evacuated", the air loss from the eye to the eyewall can therefore be more important, so that the eye's volume decreases faster, the eyewall contracts faster and the storm intensifies. As the storm approaches the trough and as the jet to east changes orientation (from North-West to South-East), the outflow of Lili is more constrained and the storm starts to feel the vertical wind shear induced by the trough and weakens.

Sensitivity experiments using different micro-physics will be performed. Further analysis with very high resolution (0.55 km) is currently underway to determine if the limitation of the numerical model represent a shortcoming to more contraction of the eye/eyewall region. Some budget analysis on the key dynamics and thermodynamics diagnostic variables at this resolution will also be performed.

Acknowledgements. The author wish to thank Dr. Shuyi Chen. The author also wish to thank NASA for the TRMM (TMI and PR) data. This work was supported by a research grant from the Office of Naval Research (N00014-01-1-0156).

REFERENCES

Black, M. L., J. E. Gamache, F. D. Marks Jr., C. E. Samsury, and H. E. Willoughby, 2002: Eastern Pacific Hurricane Jimena of 1991 and Olivia of 1994 : The effect of vertical wind shear on structure and intensity. *Mon. Wea. Rev.*, **54**,2291-2312.

Bosart, L. F., C. S. Velden, W. E. Bracken, J. Molinari, and P. G. Black, 2000 : Environmental influences on the rapid intesification of Hurricane Opal (1995) over the Gulf of Mexico. *Mon. Wea. Rev.*, **128** ,322-352.

Colon, J., A., and Lt. Cdr. W. R. Nightingale, 1963 : Development of tropical cyclones in relation to circulation patterns at the 200-millibar level. *Mon. Wea. Rev.*, **93** ,329-336.

Frank W. M. and E. A. Ritchie, 1999 : Effects of environmental flow upon tropical cyclone structure. *Mon. Wea. Rev.*, **127**,2044-2061.

Frank W. M. and E. A. Ritchie, 2001 : Effects of vertical wind shear on the intensity and structure of numerically simulated hurricanes. *Mon. Wea. Rev.*, **129**,2249-2269.

Kimball, S. K., and J. L. Evans, 2002 : Idealized numerical simulations of hurricane-trough interaction. *Mon. Wea. Rev.*, **130**,2210-2227.

Liu, Y., D..-L. Zhang, and M. K. Yau, 1997 : A multiscale numerical study of Hurricane Andrew (1992). Part I : An explicit simulation. *Mon. Wea. Rev.*, **125**,3073-3093.

Molinari, J. and D. Vollaro, 1989 : External influences on hurricane intensity. Part I : Outflow layer eddy angular momentum fluxes. *J. Atmos. Sci.*, **46**, 1093-1105.

Molinari, J., S. Skubis and D. Vollaro, 1995 : External influences on hurricane intensity. Part III : Potential vorticity structure. *J. Atmos. Sci.,* **52**, 3593-3606.

Molinari, J., S. Skubis, F. Alsheimer, and H. E. Willoughby, 1998 : Potential vorticity analysis of tropical storm intensification. *J. Atmos. Sci.,* **55**, 2632-2644.

Rogers R. S. S. Chen, J. E. Tenerelli and H. E. Willoughby 2003 : A numerical study of the impact of vertical shear on the distribution of rainfall in hurricane Bonnie (1998). *Mon. Wea. Rev.*, **131**,1577-1599.

Shi , J. J., S. W. Chang, and S. Raman, 1990 : A numerical study of the outflow layer of the tropical cyclone. *Mon. Wea. Rev.*, **118**,2042-2055.

Tenerelli J. E. and S. S. Chen, 2001 : High-resolution simulation of Hurricane Floyd (1999) using MM5 with a vortex-following mesh refinements. *Preprints, 18th Conference on Weather Analysis and Forecasting/ 14th Conference on Numerical Weather Prediction, 30 July-2 August 2001, Ft-Lauderdale, Florida*, *AMS*, J54-J56.

Willoughby, H. E. 1998 : Tropical cyclone eye dynamics. *Mon. Wea. Rev.*, **126**,3053-3067.